PHYSICAL REVIEW B VOLUME 2, NUMBER 8 15 OCTOBER 1970

Effect of Point Defects in Copper on the Anomalous Transmission of X Rays*

L. S. Edelheit,† J. C. North,‡ J. G. Ring,§ and J. S. Koehler
Department of Physics and Materials Research Laboratory, University of Illinois, Urbana, Illinois 61801

and

F. W. Young, Jr.
Solid State Division, Oak Ridge National Laboratory, Oak Ridge, Tennessee 37830
(Received 20 April 1970)

Anomalous x-ray transmission (Borrmann) measurements were made at 4.2 °K on nearly perfect copper single crystals before and after irradiation at 20 °K with 3-MeV electrons (total integrated flux 0.87×10^{18} electrons/cm^2). The intensity in the diffracted direction was measured for the (111), (222), (333), and (220) reflecting planes. The measured intensity changes were (1.2 ± 0.4)%, (4.5 ± 0.6)%, (8.9 ± 0.8)%, and (4.1 ± 0.8)%, respectively. The observed intensity changes are consistent with predictions if it is assumed that the damage consists of isolated interstitials and vacancies. Possible configurations of the interstitial are discussed. Measurements after annealing at 80 and 300 °K were made. The measurements are consistent with small defect clusters forming when the irradiated crystal was heated to 80 °K, and some clusters remaining after annealing at room temperature.

I. INTRODUCTION

Dynamical diffraction of x rays is a powerful tool for investigating defects in nearly perfect crystals. Dislocations and large defect clusters can be photographed directly by means of x-ray transmission topography. Smaller defects can be investigated by integrated intensity measurements of anomalously transmitted x rays (Borrmann effect). The clustering of oxygen in dislocation-free silicon[1] can reduce the anomalous x-ray transmission by 2 orders of magnitude. Efimov and Elistratov[2] and Maruyama[3] have investigated the effects of impurities and vacancies in germanium on Borrman intensities. Defect clusters produced in germanium and silicon by fast neutron bombardment attenuate the anomalously transmitted intensity.[4,5] In copper, Baldwin *et al.*[6] found that changes in Borrmann intensities of several orders of magnitude resulted from irradiation with 4×10^{19}/cm^2 fast neutrons. Recently, Batterman[7] has determined the position occupied by impurity atoms in a silicon lattice by measuring the x-ray fluorescence of the impurity during a dynamical diffraction process.

The present experiment was undertaken to determine the geometrical nature of a copper interstitial in a copper lattice. The previous measurements made in order to study single interstitials in copper have primarily been low-temperature measurements of resistivity and stored energy.[8] These determine the existence of the defect, but do not give much information about the atomic configuration of the interstitial. Several models of the interstitial have been proposed.[9–14] In these models the point atoms interact with two-body forces. A computer calculation then minimizes the energy associated with the various configurations. In the models, the coordinates of the atoms near the defect are considered explicitly, while the remainder of the crystal is treated as an elastic continuum which is appropriately joined to the discrete atomic arrangement used near the interstitial. The various calculations agree in that the split ⟨100⟩ interstitial has the smallest formation energy and is, therefore, the most stable. Some of the calculations, however, indicate that the formation energies of four or five contending configurations lie within 10% of the split ⟨100⟩ value. The variations in the calculated energies can be that large, depending upon the form and hardness of the interatomic potential chosen and the number of atoms which are treated as individual particles in the calculations. Furthermore, the calculations do not take into account the electron redistribution in a very realistic manner. In addition, any possible influence of *d*-electron redistribution is neglected in all calculations.

Anomalous x-ray transmitted intensity is very sensitive to the position of an atom in the unit cell, and thus can be used to experimentally determine the configuration of the interstitial and its surrounding atoms. In addition, contrary to electrical resistivity measurements, anomalous transmission is very sensitive to the clustering of interstitials and, therefore, can yield much information concerning the annealing processes in copper.

II. DESCRIPTION OF WAVE FIELDS

Anomalous transmission of x rays was first ob-

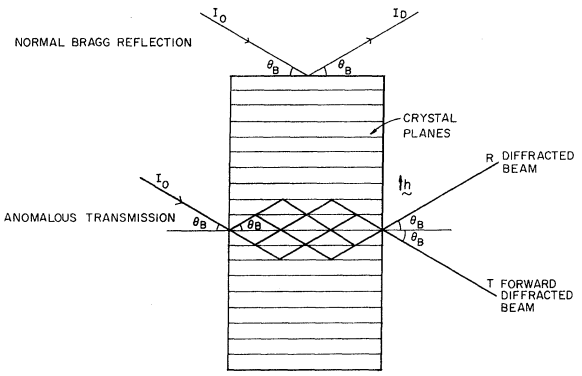

FIG. 1. Geometry of the beams when anomalous transmission is occurring. When the beam emerges from the back face, it splits into two beams, one in the forward direction, and one in the diffracted direction. The energy in the beam flows along the atomic planes in the crystal.

served by Borrmann,[15] who noted that the apparent absorption coefficient of x rays in crystals is greatly reduced for x rays incident at the Bragg angle. The theory of the diffraction of x rays through thick absorbing perfect crystals has been reviewed by several authors.[16,17] The configuration is shown in Fig. 1. A plane wave is incident on the crystal at the Bragg angle θ_B as shown. The "two-beam" case is assumed where the only other wave excited in the crystal is in a single diffracted direction. The total electric field inside the crystal is then the sum of the two coherent plane waves

$$\vec{E}(\vec{r},t)=\vec{E}_0 e^{i(\omega t-\vec{K}_0\cdot\vec{r})}+\vec{E}_H e^{i(\omega t-\vec{K}_H\cdot\vec{r})}, \quad (1)$$

where $\vec{E}_0$ and $\vec{E}_H$ are the electric field vectors of the incident and diffracted waves, respectively, and $\vec{K}_0$ and $\vec{K}_H$ are the incident and diffracted wave vectors. The wave vectors satisfy the Bragg condition $\vec{K}_0-\vec{K}_H=\vec{h}$, where $\vec{h}$ is the reciprocal-lattice vector for the diffracting planes in question,

$$\vec{h}=(4\pi\vec{n}/\lambda)\sin\theta_B, \quad (2)$$

where

$$\vec{n}=(h\vec{i}+k\vec{j}+l\vec{z})/(h^2+k^2+l^2)^{1/2} \quad (3)$$

is the unit normal to the (hkl) planes.

The time-averaged field intensity $\frac{1}{2}\vec{E}\vec{E}^*$ is

$$\tfrac{1}{2}|\vec{E}|^2=\tfrac{1}{2}[|\vec{E}_0|^2+|\vec{E}_H|^2+2\vec{E}_0\cdot\vec{E}_H\cos(\vec{h}\cdot\vec{r})]. \quad (4)$$

In anomalous transmission $|\vec{E}_0|=|\vec{E}_H|$ and the intensity becomes

$$\tfrac{1}{2}|\vec{E}|^2=|\vec{E}_0|^2[1\pm P\cos(\vec{h}\cdot\vec{r})], \quad (5)$$

where $\vec{E}_0\cdot\vec{E}_H=P|\vec{E}_0|^2$, and where $P=1$ if the incident electric field is polarized perpendicular to the incident direction (σ polarization) and $P=\cos 2\theta_B$ if the field is polarized in the plane of incidence (π polarization). For both states of polarization, the Poynting vector $\vec{E}\times\vec{H}^*$ gives an average energy flow along the atomic planes. The ($\pm$) sign takes into account the two cases in which the two plane waves have relative phases of zero or π. The branch with the minus sign is called the α branch; the branch with the plus sign is the β branch.

The expression for the field intensity shows how anomalous transmission can occur. The photoelectric absorption of an atom is proportional to the electric field intensity at the atom. If the nodal planes of the electric field ($\vec{h}\cdot\vec{r}=2n\pi$) are coincident with the atoms which make up the diffracting planes, much smaller than normal absorption takes place. It is apparent that only the σ polarization of the α branch has nodal planes at the atomic sites. In a thick crystal this is the only beam which emerges from the back face of the crystal, and therefore, we need only consider the case

$$\tfrac{1}{2}|\vec{E}|^2=|\vec{E}_0|^2[1-\cos(\vec{h}\cdot\vec{r})]=\vec{E}_0^2[1-\cos(2n\pi y/d_{hkl})], \quad (6)$$

where n is the order of reflection, d_{hkl} is the distance between the crystal planes, and y is a coordinate perpendicular to the crystal planes ($y=0$ occurs at a particular crystal plane, $y=d_{hkl}$ at the next plane, etc.).

III. EFFECTS OF DISPLACED ATOMS

For x rays incident on a crystal of thickness t at an angle θ, not satisfying Bragg's law, the emerging intensity is given by

$$I(t)=I_0\exp(-\mu_0 t/\cos\theta), \quad (7)$$

where $\mu_0=\sigma_0 N_0$ is the linear absorption coefficient, σ_0 is the normal atomic photoelectric absorption cross section, and N_0 is the number of atoms per unit volume.

With reference to Fig. 2, $\sigma(\vec{r}_a)dv$ is the photoelectric absorption cross section of the volume element dv, i.e.,

$$\sigma_0=\int_v\sigma(\vec{r}_a)dv. \quad (8)$$

Since the absorption is proportional to the time average of the intensity $\frac{1}{2}|\vec{E}|^2$, the effective atomic absorption cross section of an atom centered at $\vec{r}_a$ in the case of anomalous transmission is given by

$$\sigma^*(\vec{r}_0)=\int(\tfrac{1}{2}|\vec{E}(\vec{r})|^2/|\vec{E}_0|^2)\sigma(\vec{r}_a)dv. \quad (9)$$

It is assumed that the absorption by the atom at $\vec{r}_0$ does not distort the shape of the intensity $|E(\vec{r})|^2$. This is a good assumption for atoms and clusters whose dimensions are much smaller than an extinc-

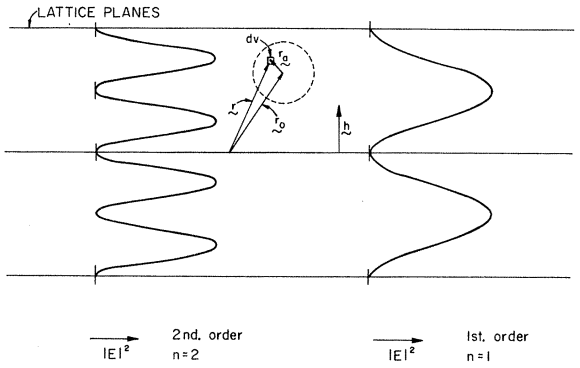

FIG. 2. Geometry used to calculate the absorption of an atom in the anomalous transmission standing-wave pattern. The absorption depends greatly on the order of reflection.

tion length ($\sim 1\ \mu$). Substituting from Eq. (6) gives

$$\sigma_h^*(\vec{r}_0) = \int \{1 - \cos[\vec{h} \cdot (\vec{r}_0 + \vec{r}_a)]\} \sigma(\vec{r}_a)\, dv . \quad (10)$$

Expanding the cosine function and noting that spherical symmetry of the atom implies that $\sigma(\vec{r}_a) = \sigma(-\vec{r}_a)$, sine term vanishes yielding

$$\sigma_h^*(\vec{r}_0) = \sigma_0 \left(1 - \frac{\cos(\vec{h} \cdot \vec{r}_0)}{\sigma_0} \int \cos(\vec{h} \cdot \vec{r}_a)\, \sigma(\vec{r}_a)\, dv\right). \quad (11)$$

If the atom is at a lattice site, $\vec{h} \cdot \vec{r}_0 = 2\pi n$ and

$$\sigma_h^*(0) = \sigma_0 (1 - \int \cos(\vec{h} \cdot \vec{r}_a)\, \sigma(\vec{r}_a)\, dv/\sigma_0). \quad (12)$$

The effective atomic absorption cross section for a lattice site atom in the case of anomalous transmission can also be written as[16]

$$\sigma^*(0) = \sigma_0(1 - \epsilon_h) , \quad (13)$$

where $\epsilon_h = f''_{hkl}(\theta_B)/f''_0(\theta_B)$ is the ratio of the imaginary part of the scattering amplitudes in the (hkl) and the forward directions. It has been shown[18–20] that $\epsilon_h = \epsilon_{0h} e^{-M}$, where M is the Debye-Waller factor. Experimental determinations of ϵ_h have been made[16] and Wagenfeld[20] has made quantum-mechanical calculations of ϵ_{0h}. Wagenfeld's results have been applied to copper,[19] yielding good agreement with experiment. Comparing Eqs. (12) and (13) shows that

$$\int [\cos(\vec{h} \cdot \vec{r}_a)\, \sigma(\vec{r}_a)\, dv/\sigma_0] = \epsilon_h . \quad (14)$$

The effective absorption cross section of an atom at $\vec{r}_0$ can therefore be written

$$\sigma_h^*(\vec{r}_0) = \sigma_0[1 - \epsilon_h \cos(\vec{h} \cdot \vec{r}_0)] . \quad (15)$$

The change in cross section, $\Delta\sigma_h^*(\vec{r}_0)$, due to moving an atom from a lattice site to a displaced position $\vec{r}_0$, is given by

$$\Delta\sigma_h^*(\vec{r}_0) = \sigma_h^*(\vec{r}_0) - \sigma_h^*(0) = \sigma_0\epsilon_h[1 - \cos(\vec{h} \cdot \vec{r}_0)] . \quad (16)$$

To get the net change in the anomalous transmission due to an interstitial-vacancy pair, we must also consider the atoms around the interstitial and vacancy which are displaced from their lattice sites. If we assume that the interstitials are randomly distributed in the lattice, and are far enough apart that the displacement of a lattice atom is due to a single interstitial, we obtain

$$\Delta\sigma_{h\,\mathrm{net}}^* = \sigma_0\epsilon_h \textstyle\sum_j [1 - \cos(\vec{h} \cdot \vec{r}_{0j})] , \quad (17)$$

where the sum is over all atoms that have been displaced by a single interstitial-vacancy pair (including the interstitial atom itself). The total absorption coefficient for a sample containing N_i interstitials per unit volume is thus larger by a term

$$\mu^* = \Delta\sigma_{h\,\mathrm{net}}^* N_i . \quad (18)$$

If $C_i = N_i/N_0$ is the concentration of interstitials, we have

$$\mu^* = \mu_0\epsilon_h C_i \textstyle\sum_j [1 - \cos(\vec{h} \cdot \vec{r}_{0j})] . \quad (19)$$

The fractional change of the transmitted intensity due to these defects for symmetric Laue geometry is

$$\frac{\Delta I}{I} = (e^{-\mu^* t/\cos\theta_B} - 1)$$
$$\simeq \frac{-\mu_0 t}{\cos\theta_B} \epsilon_h C_i \sum_j [1 - \cos(\vec{h} \cdot \vec{r}_{0j})] . \quad (20)$$

The expansion is good for small concentrations of interstitials.

It is apparent that anomalous transmission is sensitive to the displacements $\vec{r}_{0j}$. If we consider the expression $\cos(\vec{h} \cdot \vec{r}_{0j}) = \cos(2n\pi y/d_{hkl})$, we see that for an atom halfway between the planes [1 $-\cos(2n\pi y/d_{hkl})$] equals two for the first-order reflection ($n = 1$), and zero for the second-order reflection ($n = 2$). This is shown in Fig. 2. Thus for a "body-centered" interstitial atom the absorption in the first order is much larger than in the second order.

In gold[21] and silver,[22] Shimomura has shown that after electron irradation at 130 °K one sees interstitial loops by electron microscopy done below the temperature associated with stage III. He finds that the clusters become smaller as one anneals through stage III. Recently, Haussermann, Ruhle, Roth, and Scheldler[23] have shown by electron microscopy that clusters exist at 300 °K in copper irradiated at 150 °K.

The effect of clusters and dislocation loops on the anomalous transmission of x rays has been treated by Dederichs,[24,25] and by Young, Baldwin, and Dederichs,[26] who used the displacement field of a loop in an isotropic elastic solid, and find[26] that

$$\Delta I/I \propto C_l (bh)^{3/2} R_0^3 , \quad (21)$$

where C_l is the concentration of independent loops, b is the Burgers's vector (perpendicular to the loop plane), and R_0 is the radius of the loop. If C_i is the concentration of interstitials, then $C_l \propto C_i/R_0^2$, and for a given crystal reflection

$$\Delta I/I \propto C_l R_0^3 \propto C_i R_0 \,. \tag{22}$$

Therefore, for a given number of interstitial atoms, the change in intensity is proportional to the radius of the clusters into which the interstitials are formed.

Dederichs[24-26] treats the entire problem of the effect of point defects on anomalous transmission by considering the scattering to be from an effective optical potential. He develops a generalized Debye-Waller function including the displacements due to defects as well as due to thermal vibrations.

This treatment leads to the same result as in Eq. (20). He also considers the effect of diffuse scattering by defects in which the scattered x ray does not satisfy Bragg's condition and is, therefore, absorbed by the crystal. The diffuse scattering is wavelength dependent and is very sensitive to the clustering of defects. He finds[25] that for Mo$K\alpha$ x rays this is a small effect if the clusters present in the electron-irradiated copper are not too large. Since below 20 °K the damage consists of single interstitials and vacancies, the diffuse scattering term may be neglected. After annealing this term should be taken into account.

IV. EXPERIMENTAL PROCEDURES

Single crystals of (99.999+)% copper were grown by methods described previously.[27] A $1\times1\times2$-cm parallelopiped was cut from a crystal by an acid saw,[28] annealed at 1075 °C for about two weeks to eliminate dislocations, and irradiated with 10^{17} *nvt* fast neutrons at a temperature below 100 °C to pin the remaining dislocations and minimize damage due to handling. The effect on the anomalous transmission due to this irradiation is small[29] and it is assumed to remain constant during the experiment. The parallelopiped was sliced into $1\times1\times t$-cm pieces (t between 0.025 and 0.205 cm). Two adjacent slices having (110) faces to within 0.5° were polished and electropolished[28] to eliminate surface damage.

The thickness of the crystals was determined by absolute integrated intensity measurements, and also by the relative intensities of various orders of reflection. The electron irradiated crystal was 0.9 ± 0.1 mm thick while the unirradiated reference crystal was 0.8 ± 0.1 mm thick. Because of the polishing process, the crystal faces were slightly convex. The measurements were made at the flattest part of the crystals.

X-ray topographs were taken. They showed a few dislocations in the corners of of the crystals, but none in the central regions where the intensity measurements were made.

Although the presence of neutron irradiation damage permitted handling of the crystals, Penning and Polder,[30,31] Hunter,[32] and others have shown that strains of very small magnitude can be detected by anomalous transmission. Since the measurements were made at very low temperatures, mechanical strains due to differential thermal contractions could have reduced the diffracted x-ray intensity drastically if the crystals were rigidly supported. Thus the crystals were placed in a copper holder, as shown in Fig. 3, with approxi-

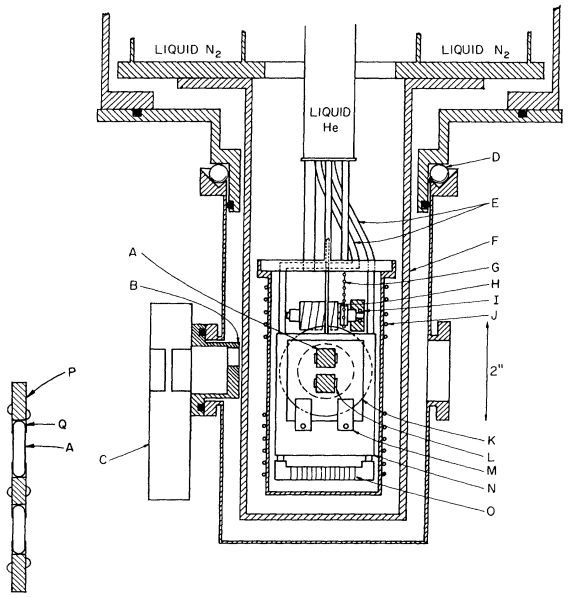

FIG. 3. Sectional view of the specimen chamber: (A) two copper crystals to be measured: irradiated specimen and unirradiated reference crystal; (B) $\frac{1}{4}$-in.-thick brass aperture for electron beam; (C) valve for connection to van de Graaff; (D) ball-bearing race to rotate outer chamber; (E) 0.010-in. wall inconel tubes conducting liquid helium to sample chamber, flow control valve not shown; (F) liquid-nitrogen temperature radiation shield, aluminum-coated Mylar windows not shown; (G) $\frac{3}{32}$-in.-diam stainless-steel bead chain wrapped around a sprocket; (H) worm gear; (I) miniature ball bearing (only one shown); (J) "Xactglo" heating element soldered to sample chamber, Dural windows not shown; (K) worm wheel for rotation; (L) cut outs in sample mount used to locate the crystal position; (M) copper posts used to align the electron beam with respect to the sample; (N) $\frac{3}{16}$-in. copper shield which can be raised from above to shield the lower copper crystal from electron irradiation; (O) copper heat exchanger with fins through which the liquid helium flows to cool the helium exchange gas. The insert is a side view of the sample holder showing: (A) two samples; (P) the copper sample mount; (Q) Be-Cu strips to keep samples from falling out.

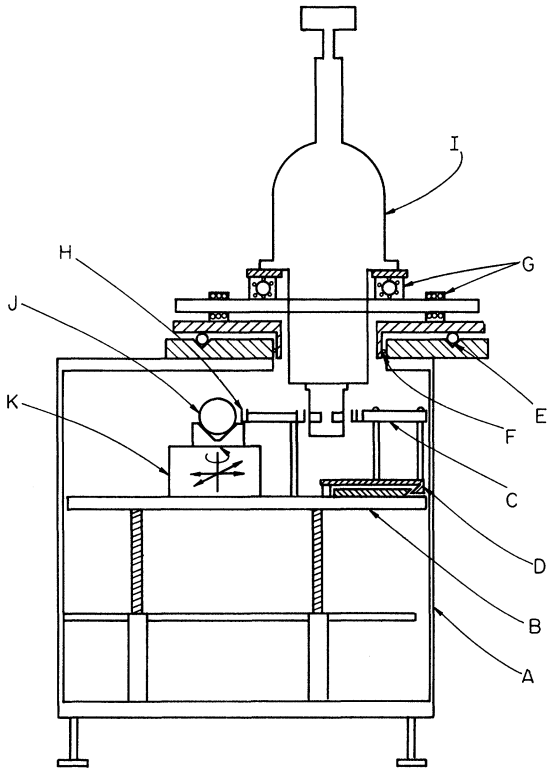

FIG. 4. Schematic diagram of x-ray apparatus; (A) table which supports entire structure; (B) elevating table to raise the x-ray tube and detector with respect to the crystal (i.e., adjusts z position); (C) detector and preamplifier; (D) dovetail to provide rotation of the detector; (E) ball-bearing race for the θ rotation of cryostat; (F) bearing to keep the center of the θ rotation fixed; (G) ball bushings and rods for translating cryostat in x and y directions; (H) holders for x-ray apertures and absorbers (4-in. view); (I) 5-liter helium cryostat. The x-ray tube (J) is positioned by the base (K) which provides linear motion in the horizontal plane, and rotation around a vertical axis.

mately 0.005-in. clearance on all sides. The only external force on the crystals was due to gravity. Thin (0.005-in.) Be-Cu strips prevented the crystals from falling out of the mount. The $\frac{3}{16}$-in. copper shield allowed the upper crystal to be irradiated, but protected the lower crystal from electron damage. The samples could be rotated 360° about the normal to the crystal face (φ rotation).

The sample temperature was measured by means of a carbon resistor, and all x-ray measurements were made at $T < 5$ °K.

The x-ray system and cryostat are shown schematically in Fig. 4. The system allowed the x-ray beam to be moved in the z direction and the samples to be moved in the x and y directions. These coordinates were measured with dial indicators to the nearest 0.01 mm. A series of lever arms and a micrometer gauge permitted changes in the θ angle (Bragg angle) of 1 sec of arc to be measured and the angle φ could be set to 0.1°.

The x-ray power supply was a GE XRD-6 unit with a constant potential assembly and voltage stabilizer to minimize power fluctuations. A molybdenum target x-ray tube was used, and the sample was adjusted for the $K\alpha$ reflection.

No monochromator was used in the system. This precluded making absolute integrated intensity measurements. However, since the primary interest was the change of the x-ray intensity, an absolute integrated intensity determination was not necessary. Furthermore, the monochromators tested introduced nonuniformities in the x-ray beam that led to variations in the measurements beyond our required precision.

The intensity measurements were made using a NaI(Tl) detector. A single-channel analyzer discriminated against $\frac{1}{2}\lambda$ radiation and a 0.006-in. aluminum filter in front of the detector reduced the number of low-energy x rays to a negligible contribution. The amplification and pulse-height analysis components of the counting system were enclosed in a constant temperature cabinet (±1 °C) to minimize the temperature effects of these components. Counts of Fe^{55} decay up to 10^7 were consistent within statistics (~0.03%) over periods of days.

Measurements were made at two locations on the unirradiated reference crystal and one location on the irradiated crystal. Because of sample-thickness variations, the same locations were always used and were relocated to ±0.03 mm. The x-ray-beam diameter at the crystal was 2 mm. All intensity measurements were made by maximizing the counting intensity for Mo$K\alpha$ x rays. This peak intensity was then measured. Since no monochromator was used some x rays other than Mo$K\alpha$ are transmitted; however, their number is small, and the same for both unirradiated and irradiated crystals. At the peak the change in counting intensity from the peak value to 99% of the peak value was smooth and corresponded to a change in θ of 200″. The location of the peak was determined to 3″, corresponding to about 0.01% change in intensity.

The effect of long-range strains on the anomalous transmission intensity was minimized by using the average intensity of the (hkl) and $(\bar{h}\bar{k}\bar{l})$ reflections. This has been justified[30,31] and will be discussed quantitatively in Sec. VI.

Measurements were taken before irradiation, after irradiating with 0.43×10^{18} e/cm^2, and again after 0.87×10^{18} e/cm^2. The crystals were then annealed at 78 °K for 48 h and remeasured. Finally the crystals were measured after annealing at 300 °K for 48 h. All measurements were made at

liquid-helium temperature. The first three orders of the (111) planes and the first order of the (220) planes were measured although the (220) and (333) preirradiation measurements were not taken. In these two cases, the damage production was assumed to be proportional to flux [which is true for the (111) and (222) reflections]. To check reproducibility the measurements were made twice after the irradiation of 0.43×10^{18} e/cm^2, and the results agreed within experimental error.[33]

The (3.0 ± 0.1)-MeV electron-beam current was ~ 0.35 $\mu A/cm^2$, and the sample temperature during irradiation was kept below 22 °K. The total irradiation time was 120 h with a total flux of 0.87×10^{18} e/cm^2. After fluxes of 0.21 and 0.64×10^{18} e/cm^2, the cryostat was rotated 180° so that the electron beam was incident on the opposite face of the crystal. This was done to reduce the strains in the crystal due to defect concentration gradients. Since the electrons lost about 1.0 MeV in traversing the crystal, the total displacement cross section (including secondary displacements) went from about 120 b at the entering face to about 90 b at the exit face assuming a displacement threshold energy of 22 eV.[34] Thus, the concentration of defects was less at the back surface of the crystal than at the front surface. This was partially compensated for by the Yang correction[8] because the path length (and hence the damage production) was larger near the back face due to multiple scattering. Because of the neutron hardening, the strain due to the defect concentration gradient will be elastic for reasonably small concentrations. By irradiating with half the flux incident on one surface and half the flux incident on the opposite surface, the concentration gradients were made smaller. Calculations show that the defect concentration was a maximum at the center of the crystal, and the difference from the center to either surface was about 3%. This was not large enough to affect the anomalous transmitted intensity.

V. EXPERIMENTAL RESULTS

The intensity of anomalously transmitted x rays was normalized by taking the ratio of the count rate for the irradiated crystal to the count rate at one location on the unirradiated reference crystal. The percentage change of this ratio as a function of irradiation fluence and subsequent isochronal annealing temperature is shown in Fig. 5. The values plotted are the changes of the averages of the (hkl) and $(\bar{h}\bar{k}\bar{l})$ reflections.

There were three sources of errors in the experiment. The first source was the change in intensity due to strains in the irradiated crystal which might have changed during the irradiation. This was a small effect and will be discussed in Sec. VI. A

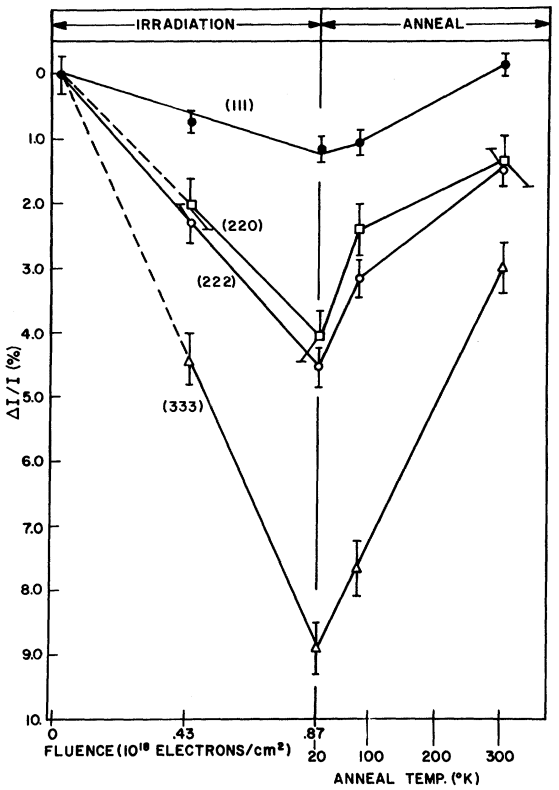

FIG. 5. Change in the anomalously transmitted x-ray intensity for four sets of reflecting planes as a function of the 3-MeV electron fluence and the subsequent isochronal annealing temperature.

second source of error arises from fluctuations of x-ray-tube voltage, changes in room temperature with time, counting statistics, errors in the determination of angle or position, etc. Errors of this type would be the same in the unirradiated crystal as in the irradiated crystal. Thus, by measuring the changes in the ratio of the two locations on the unirradiated crystal throughout the experiment, we obtained the error (standard deviation) present due to all such factors. For example, six measurements of this ratio in the (222) configuration made over a 4-month period gave a standard deviation of $\pm0.2\%$, the largest deviation being 0.3%. The third source of error is due to shifting of the crystals in the mount. The location of the crystals was determined to ±0.03 mm and the change in intensity as a function of position near the locations was carefully measured. Thus, the error due to uncertainty in position was determined. The values for all three sources of error are shown in Table I.

VI. CALCULATIONS AND DISCUSSIONS

Five possible equilibrium configurations of the

TABLE I. Experimental errors associated with each data point of Fig. 5.

Reflecting planes	Standard deviation of counting statistics (%)	Positioning of beam on crystal (%)	Strain	Total error (%)
(111)	±0.1	±0.1	0	±0.2
(222)	±0.2	±0.1	0	±0.3
(333)	±0.2	±0.1	±0.1	±0.4
(220)	±0.25	±0.15	0	±0.4

interstitial have been considered in the calculations, where the notation is that of Seeger *et al.*[10] and Johnson.[14] The energies and displacements associated with these configurations have been treated theoretically using a wide variety of models. Johnson[35] points out that these calculations are essentially computer "experiments," and a comparison of the models involves a discussion of accuracy. For example, the results depend critically on the computational cell size. In region 1, the displaced atoms are close to the center of the interstitial configuration and the atoms cannot be adequately described in terms of linear elastic theory. The displacements are large and the atoms must be treated as discrete particles. Several authors[9–14] have published calculations. The resulting displacements can be put directly into the sum of Eq. (20). The results are shown in Table II. In each case it is assumed that the interstitials are isotropically distributed over all possible orientations (e.g., the ⟨100⟩ split in interstitial can lie along three different ⟨100⟩ directions).

The number of atoms included in region 1 and the distance of the most distant region-1 atom from the interstitial ($r_{\min}$) are also shown in Table II.

The displacement of atoms in the elastic continuum (region 2) must also be considered in the calculations. In continuum theory, assuming an isotropic medium, the displacement field of an "isotropic" point defect is

$$\vec{r}_{0j}(\vec{r}) = A\,\vec{r}/r^3 \quad , \tag{23}$$

where $\vec{r}_{0j}(r)$ is the displacement of atom j which is located at a distance $\vec{r}$ from the defect. The quantity A is related to the volume change ΔV by

$$\Delta V = 4\pi A\, 3(1-\nu)/(1+\nu) \, , \tag{24}$$

where ν is Poisson's ratio.

In region 2, the displacement r_{0j} is small and the sum in Eq. (20) becomes

$$\textstyle\sum_j [1-\cos(\vec{h}\cdot\vec{r}_{0j})] \cong \sum_j \frac{1}{2}(\vec{h}\cdot\vec{r}_{0j})^2 . \tag{25}$$

If we convert the sum to an integral over region 2, which includes all atoms farther from the interstitial than a minimum distance $r_{\min}$, we get

$$\sum_j [1-\cos(\vec{h}\cdot\vec{r}_{0j})] \cong \frac{2}{3}\pi \frac{A^2|h|^2}{r_{\min}} \frac{4}{a^3} \, , \tag{26}$$

where a is the lattice constant, and there are $4/a^3$ atoms per unit volume. If we assume $\nu = \frac{1}{3}$ for copper, and $\Delta V = \frac{1}{2}a^3 \cong$ two atomic volumes for a single interstitial,[36] we get

$$A = 0.03a^3 \tag{27}$$

and

$$\sum_j [1-\cos(\vec{h}\cdot\vec{r}_{0j})] \cong \frac{0.3a}{r_{\min}}(h^2+k^2+l^2) \, . \tag{28}$$

These values are also given in Table II. Thus the contribution to Eq. (20) from all atoms farther from the interstitial than $r_{\min}$ is

$$\left(\frac{\Delta I}{I}\right)_{\text{region 2}} = \frac{\mu_0 t}{\cos\theta_B} \epsilon_h C_i \frac{0.3a}{r_{\min}}(h^2+k^2+l^2) \, . \tag{29}$$

In each case, region 2 is taken to be the atoms not

TABLE II. Effect of displaced atoms in regions 1 and 2 on the anomalous transmission of x rays for five models of the isolated interstitial and the vacancy. Equation (28) is used for region 2. 0 is the body-centered configuration which has octahedral symmetry; H_0 is the ⟨100⟩ split configuration; H_T is the ⟨111⟩ split configuration; H_c is the ⟨110⟩ split, or split crowdion configuration; and T is the tetrahedral symmetry configuration.

Type of defect	Displacements used	Number of atoms in region 1	$r_{\min}/a$	$\sum_j [1-\cos(\vec{h}\cdot\vec{r}_{0j})]$ Reflecting Planes 111 Reg. 1	111 Reg. 2	222 Reg. 1	222 Reg. 2	333 Reg. 1	333 Reg. 2	220 Reg. 1	220 Reg. 2
0	Johnson (Ref. 43)[a]	267	2.5	3.11	0.32	7.85	1.28	17.67	2.88	5.23	0.84
H_0	Johnson (Ref. 43)[a]	250	2.4	3.89	0.34	8.65	1.34	10.19	3.02	5.97	0.88
H_T	Doyama (Ref. 11)	53	1.4	3.48	0.57	8.03	2.27	13.72	5.11	5.78	1.49
H_c	Doyama (Ref. 11)	56	1.2	3.56	0.66	5.50	2.66	8.08	5.98	6.53	1.74
T	Doyama (Ref. 14)	71	1.6	3.67	0.50	9.54	2.02	12.85	4.54	5.88	1.32
Vacancy	Doyama (Ref. 11)	54		0.131		0.519		1.15		0.412	

[a]Using displacements associated with the intermediate-range potential as explained in an unpublished paper.

TABLE III. Decrease in transmitted intensity $\Delta I/I$ in % due to interstitial-vacancy pairs.

			Calculated (based on $C_i = C_v = 1.2 \times 10^{-4}$ Type of interstitial					
hkl	ϵ_{0h}	e^{-M}	0	H_0	H_T	H_c	T	Experiment
111	0.998	0.991	1.65	2.03	1.93	2.02	1.99	1.2 ± 0.4
222	0.993	0.996	4.56	4.96	5.11	4.09	5.70	4.5 ± 0.6
333	0.985	0.926	10.63	7.04	9.79	7.45	9.08	8.9 ± 0.8
220	0.995	0.997	3.04	3.40	3.60	4.07	3.56	4.1 ± 0.8

included in the calculation of region 1.

Several approximations have been made in deriving this equation. The copper lattice is not isotropic. Thus the displacement field should be represented by a more complicated expression.[37] Also, the field around several of the configurations shows other than spherical symmetry (e.g., the ⟨100⟩ split interstitial). There are also corrections to the displacement field of order $1/r^4$. The volume change ΔV is not accurately known and may be different for different interstitial configurations.

The choice of this one term as the only contribution to the elastic displacement field is discussed in detail by Johnson and Brown[9] who point out that the atomic configurations near defects are insensitive to other solutions of the isotropic elastic equation, and it has been shown[38] that anisotropic solutions do not play a large role. Since region 2 represents only a small part of the total intensity change, the isotropic elastic solution is probably a valid approximation.

The constants in Eq. (20) have been determined. The value $\mu_0 = 438$ cm^{-1} has been measured experimentally for similar copper crystals for Mo$K\alpha$ x rays. It has been shown[16] that

$$\frac{(1-\epsilon_{0h})}{(1-\epsilon_{0h'})} = \frac{d^2_{h'k'l'}}{d^2_{hkl}} \quad . \tag{30}$$

Experimental values of ϵ_{0h} for the (111), (222), and (220) reflections have been determined[39] and fit Eq. (30) very well. These experimental values also agree with the theoretical calculations.[19] Equation (30) has been used to evaluate ϵ_{0h} for the (333) reflection. The calculated Debye-Waller factor e^{-M} is shown in Table III, using a Debye temperature of 300 °K.[40]

The concentration of interstitials C_i can be calculated from the displacement cross section. Displacement cross sections have been calculated for copper by Oen[34] using relativistic scattering theory. The calculation follows closely that of Seitz and Koehler.[41] Included in the calculations is the effect of the secondary displacements being produced. A displacement threshold energy of 22 eV was used,[8] and the Yang correction[8] was applied. The calculated average Frenkel pair concentration for a total fluence of 0.87×10^{18} e/cm^2, with half of the fluence incident on each side of the crystal is $C_i = 1.2 \times 10^{-4}$.

The effect of the vacancy on the anomalous transmission is much smaller than that of the interstitial. In the previous calculation it was assumed that the effect of an interstitial atom was the same as that of a displaced atom. Thus the "vacancy" was already included in the calculation. There is, however, a change in intensity due to atoms collapsing around the vacancy. Using the displacements of Doyama and Cotterill,[11] calculations can be made of the effect of the vacancies on the anomalous transmission. This contribution has been included in the results given below.

No calculations have been made using the fact that the displacements around a Frenkel pair are different from the displacements around isolated interstitials and vacancies. It is assumed that the displacements around the interstitials are not altered by the presence of a nearby vacancy. This seems reasonable because (a) the closest interstitial vacancy pairs are unstable[14]; (b) the close pairs associated with stage I_A are not present during irradiation at 20 °K; (c) the displacements near a vacancy are small.

The results of the calculations are shown in Table III. These results include the change due to the displaced atoms in region 1, region 2, and the displaced atoms around the vacancies. The calculations are based on a defect concentration of 1.2×10^{-4} and the values of Table II.

The best fit to the body-centered interstitial is obtained for $C_i \cong 1.1 \times 10^{-4}$. This agrees remarkably with the calculated concentration. If it is assumed that the average concentration is given reasonably well by simple displacement theory, the resistivity of a Frenkel pair can be calculated using the results of Corbett *et al.*[42] The results are $\Delta\rho = 1.4$ $\mu\Omega$ cm/at.% for copper. Thus, if the displacement calculations[9-14] are correct, the calculations[34,41] of defect concentration are consistent with the present experiment.

Stored energy, length change, and lattice parameter changes measured after 10-MeV proton and deuteron irradiation indicates that the simple displacement theory gives a much higher damage production rate than observed.[43] However, it may be that the large amount of atomic motion associated with the displacements due to the energetic primary knockons in proton or deutron irradiation causes some defect annihilation so that the simple theory is incorrect in such cases.

Several of the constants in Eq. (20), including the concentration, cancel out by considering ratios of the changes for various orders of reflection. In this way the experimental values can be compared

with the calculated values for the various interstitial models, and the uncertainty in the interstitial concentration is avoided. These ratios, calculated from both the theoretical and the experimental values of Table III, indicate that both the body-centered and the ⟨111⟩ split interstitial models are consistent with the experimental values within the experimental errors. However, the theoretical ratios for the ⟨100⟩ split interstitial model do not agree with the experimental values within the experimental errors. This is true using the displacement values of any of the authors[9–14] who treated the ⟨100⟩ split interstitial. The difference between these ratios, however, are only slightly outside of the experimental errors, and although the stated errors are probably the upper limit of the possible errors, they are not known precisely. Therefore, more samples will be measured in order to determine and possibly reduce the errors. Also the accuracy of the theoretical displacement calculations is not well known.

The change in the anomalous transmission due to strains has been discussed by Penning and Polder,[31] and by Okkerse and Penning.[30] They extend the dynamical theory of x-ray diffraction to include the case where the lattice parameter varies slowly with respect to the extinction distance. For the case where the count rate is proportional to the integrated intensity, they obtain

$$\ln(T/T_0) = -\tfrac{1}{6}P^2(C+\tfrac{3}{2}) , \tag{31}$$

$$\ln(R/T) = 2\ln[(1+P^2)^{1/2}-P] - [2(1+P^2)^{1/2}-P]C^{-1}, \tag{32}$$

where $C=(\mu_0 t/\cos\theta_B)\epsilon_h \cong 40 \gg 1$ for this experiment, R and T are the count rates in the diffracted and incident directions after straining, and T_0 is the count rate in the incident direction before straining (see Fig. 1).

P is a parameter depending on the kind of deformation of the crystal. It is also proportional to the angle the diffracting planes make with the surface of the crystal. For example, if the crystal is deformed by a bending moment,

$$P = \frac{\delta}{\Psi_h R}\tan\theta_B[1+(1+\nu)\cos^2\theta_B]t , \tag{33}$$

where δ is the small angle between the normal to the surface and the reflecting planes, R is the radius of curvature of the sample, ν is Poisson's ratio, and Ψ_h is the atomic scattering factor for the reflection under consideration. For small strains, P is small and Eqs. (31) and (32) can be expanded to give

$$R \cong R_0(1+2P+9P^2+\cdots) , \tag{34}$$

where R_0 is the intensity in the diffracted direction before straining. If the crystal is bent by the mount or by the radiation damage, or if a temperature gradient exists in the crystal, P is an odd function of θ_B and, therefore,

$$P_{\theta_B} = -P_{-\theta_B} . \tag{35}$$

Thus by taking an average of R_{hkl} and $R_{\bar{h}\bar{k}\bar{l}}$ we eliminate the effect of strain to first order in P. By taking the value of

$$4P = (R_{hkl} - R_{\bar{h}\bar{k}\bar{l}})/R_0 , \tag{36}$$

we can determine the change in intensity

$$(\Delta I/I)|_{hkl} \approx 9P^2 \tag{37}$$

due to strain. The results show that a negligible change due to strain occurs for the (111), (222), and (220) reflections but as much as 0.1% change is possible for the (333) reflection. This is less than 2% of the measured change. It is assumed, therefore, that only small point defects are causing the measured transmitted intensity changes.

The results of the annealing can only be discussed qualitatively. Studies of the recovery of electrical resistivity produced by electron irradiation of copper show that only a small fraction (≈ 20%) of the resistivity increase remains after warming to 60 °K. In addition, most of the electrical resistivity remaining at 60 °K recovers during stage-III annealing which occurs at ≈ 300 °K.

This is not the case in the x-ray measurement. Only a small amount of recovery occurs below 80 °K, and, with the exception of the first-order (111) reflection, about 30% of the induced intensity change still remains after annealing to 300 °K.

This discrepancy can be explained in terms of the clustering of defects. A cluster of interstitials forming a loop has a lower electrical resistivity than the same number of isolated interstitials. Based on experiments comparing the resistivity present after irradiation at 20 °K and subsequent anneal at 80 °K, with the resistivity present after irradiation with the same flux at 80 °K,[8] it has been argued that interstitial clustering occurs below 80 °K. Therefore, the data of the present experiment can be explained by assuming that although all of the close Frenkel pairs recombine during stage I, the remaining interstitials can form clusters causing a relatively large change in intensity. Unfortunately, neither the number of clusters nor the radius of the clusters are known. Therefore, quantitiative comparison of theory and experiment cannot be made. It is interesting to note that the recovery of the x-ray intensity change was large in the (220) and (222) reflections which is consistent with Shimomura's finding[21] that the clusters exist as dislocation loops in the (111) planes.

Haussermann *et al.*[23] have made electron micro-

scope studies of defect clusters in 3-MeV electron-irradiated copper. Although most of the irradiation was done at 120 °K and above, one measurement was made on a specimen irradiated at 15 °K. They find, upon warming to room temperature, a defect cluster concentration of 2.7×10^{-7} after a flux of 2.9×10^{19} e/cm^2. Unfortunately, the size and concentration of the clusters as a function of flux is not known for the sample irradiated at 15 °K. One would expect a much different relationship to hold for the samples irradiated below stage I, where the mechanisms of clustering are different than for samples irradiated above stage I. For example, di-interstitials may be formed upon annealing through stage I without the presence of impurities.[8] However, assuming an average cluster size of 20 Å in diameter, which is consistent with the data of Haussermann *et al.* in samples irradiated at 130 °K, and assuming that the cluster concentration is a linear function of flux for the 15 °K irradiated crystals, a cluster concentration of about 1×10^{-8} would be expected.

Results of the data of Baldwin, Sherrill, and Young[6] on fast neutron irradiation of copper indicate that for a concentration $C_1 = 6\times10^{-6}$ of dislocation loops with an average radius equal to 20 Å, the experimental value of the effective linear absorption coefficient for the (111) reflection with Mo$K\alpha$ x rays is given by

$$\mu^* \cong 4\ \mathrm{cm}^{-1}\ .$$

Thus, by using the change in intensity due to loops [Eq. (21)], we expect for the intensity change in the (hkl) reflection

$$\frac{\Delta I}{I} \cong (4\ \mathrm{cm}^{-1})\, t\left(\frac{R_0}{20\ \text{Å}}\right)^3 \frac{C_1}{6\times10^{-6}}\left(\frac{h^2+k^2+l^2}{3}\right)^{3/4}\ . \quad (38)$$

Using the values $t = 0.9$ mm, $R_0 = 10$ Å, and $C_1 = 10^{-6}$, we obtain

$$\left.\frac{\Delta I}{I}\right|_{hkl} \cong 0.7\left(\frac{h^2+k^2+l^2}{3}\right)^{3/4}\% \ . \quad (39)$$

This does not agree with the results of the (111) reflection but for the other sets of planes [i.e., (222), (333), (220)], the results agree remarkably well with the data. However, there are so many assumptions made in the calculations that it is quite fortuitous that the results agree this well. If the clusters are indeed this large, then the neglect of the diffuse scattering term is no longer justified[24-26] and may even be as large or larger than the photoelectric absorption. However, since the number and size of these defects are not known, quantitative calculations cannot be made at this time.

The fact that the intensity in the (111) reflection completely recovers is inconsistent with the results of the other reflecting planes, and cannot be explained at this time.

VII. SUMMARY AND CONCLUSIONS

The effect of 3-MeV electron irradiation at 20 °K and subsequent isochronal annealing of a nearly perfect copper crystal has been investigated by x-ray anomalous transmission intensity measurements at 4.2 °K. These measurements are reproducible to ±0.4%. The change in the transmitted intensity due to the electron irradiation is linear with electron fluence within experimental errors. The observed changes in the transmitted intensity agree very well with theoretical calculations based on detailed models of the copper interstitial including the displacements of the surrounding lattice atoms. This suggests that the defect concentration given by simple displacement theory plus a Yang path length correction is good to ±20%. The results indicate that the split ⟨100⟩ interstitial may not be the stable configuration.

Anomalous transmission is very sensitive to clustering of defects. The results are consistent with small interstitial clusters forming during stage-I annealing, and partially annealing at room temperature. Strains due to large defect clusters were not observed.

ACKNOWLEDGMENTS

We wish to thank Professor R. O. Simmons for assistance in designing the experimental apparatus. We wish to express our gratitude to Dr. T. O. Baldwin for several helpful discussions during the course of the work. We also thank Dr. G. Bedendo and B. S. Brown for their assistance with the experimental apparatus.

---

*Work supported in part by the U. S. Atomic Energy Commission under Contract No. AT(11-1)-1198.

†Present address: General Electric Research and Development Center, Schenectady, N. Y.

‡Present address: Bell Telephone Laboratories, Murray Hill, N. J.

§Present address: Circle Campus, University of Illinois, Chicago, Ill.

[1]J. R. Patel and B. W. Batterman, J. Appl. Phys. 34, 2716 (1963).

[2]O. N. Efimov and A. M. Elistratov, Fiz. Tverd. Tela 4, 2908 (1962) [Soviet Phys. Solid State 4, 2131 (1963)].

[3]S. Maruyama, J. Phys. Soc. Japan 20, 1399 (1965).

[4]R. Collella and A. Merlini, Phys. Status Solidi 14, 81 (1966).

[5]T. O. Baldwin and J. E. Thomas, J. Appl. Phys. 39, 4391 (1968).

[6]T. O. Baldwin, F.A. Sherrill, and F. W. Young, Jr., J. Appl. Phys. 39, 1541 (1968).

[7]B. W. Batterman, Phys. Rev. Letters 22, 703 (1969).
[8]For a discussion, see J. W. Corbett, in *Solid State Physics*, edited by F. Seitz and D. Turnbull (Academic, New York, 1966), Suppl. 7.
[9]R. A. Johnson and E. Brown, Phys. Rev. 127, 446 (1962).
[10]A. Seeger, E. Mann, and R. J. van Jan, Phys. Chem. Solids 23, 639 (1962).
[11]M. Doyama and R. M. J. Cotterill, in *Lattice Defects and Their Interactions*, edited by R. R. Hasiguti (Gordon and Breach, New York, 1968).
[12]L. Tewordt, Phys. Rev. 109, 61 (1958).
[13]K. H. Bennemann, Z. Physik 165, 445 (1961).
[14]R. A. Johnson, Phys. Rev. 145, 423 (1966).
[15]G. Borrman, Z. Physik 127, 297 (1950).
[16]B. W. Batterman and H. Cole, Rev. Mod. Phys. 36, 681 (1964).
[17]R. W. James, in *Solid State Physics*, edited by F. Seitz and D. Turnbull (Academic, New York, 1963), Vol. 15, p. 53.
[18]P. H. Dederichs, Physik Kondensierten Materie 5, 347 (1966).
[19]Merlini and E. van der Voort, Euratom Report No. 1643, 1965 (unpublished).
[20]H. Wagenfeld, Phys. Rev. 144, 216 (1966).
[21]Y. Shimomura, Phil. Mag. 19, 773 (1969).
[22]Y. Shimomura, J. Appl. Phys. 41, 749 (1970).
[23]F. Haussermann, M. Ruhle, G. Roth, and G. P. Scheidler, Phys. Status Solidi 32, K 103 (1969).
[24]P. H. Dederichs, Phys. Status Solidi 23, 377 (1967).
[25]P. H. Dederichs (unpublished).
[26]F. W. Young, Jr., T. O. Baldwin, and P. H. Dederichs, in *Vacancies and Interstitials in Metals*, edited by A. Seeger, D. Schumacher, W. Schilling, and J. Diehl (North-Holland, Amsterdam, 1970), p. 619.
[27]F. W. Young, Jr., and J. R. Savage, J. Appl. Phys. 35, 1917 (1964).
[28]F. W. Young, Jr., and T. R. Wilson, Rev. Sci. Instr. 32, 559 (1961).
[29]R. M. Nicklow, F. A. Sherrill, and F. W. Young, Jr., Phys. Rev. 137, A1417 (1965).
[30]B. Okkerse and P. Penning, Phillips Res. Rept. 18, 82 (1963).
[31]P. Penning and D. Polder, Phillips Res. Rept. 16, 419 (1961).
[32]L. P. Hunter, J. Appl. Phys. 30, 874 (1958).
[33]L. S. Edelheit, Ph. D. thesis, University of Illinois, 1970 (unpublished).
[34]O. S. Oen, ORNL Report No. ORNL-3813, 1965 (unpublished).
[35]R. A. Johnson, J. Phys. Chem. Solids 28, 275 (1967).
[36]A. C. Damask and G. J. Dienes, *Point Defects in Metals* (Gordon and Breach, New York, 1963).
[37]K. C. Lie and J. S. Koehler, Advan. Phys. 17, 421 (1968).
[38]R. A. Johnson, J. Phys. Chem. Solids 26, 75 (1965).
[39]T. O. Baldwin, F. W. Young, Jr., and A. Merlini, Phys. Rev. 163, 591 (1967).
[40]T. O. Baldwin, Phys. Status Solidi 25, 71 (1968).
[41]F. Seitz and J. S. Koehler, in *Solid State Physics*, edited by F. Seitz and D. Turnbull (Academic, New York, 1956), Vol. 2.
[42]J. W. Corbett, R. B. Smith, and R. M. Walker, Phys. Rev. 114, 1452 (1959).
[43]R. O. Simmons, J. S. Koehler, and R. W. Balluffi, *Radiation Damage in Solids* (International Atomic Energy Agency, Vienna, 1962).

PHYSICAL REVIEW B VOLUME 2, NUMBER 8 15 OCTOBER 1970

s-Polarized Optical Properties of Metals*

K. L. Kliewer and Ronald Fuchs
Institute for Atomic Research and Department of Physics, Iowa State University, Ames, Iowa 50010
(Received 27 April 1970)

A theory for the *s*-polarized optical properties of a metallic slab of arbitrary thickness is presented. The light can be incident upon the slab at an arbitrary angle of incidence, and it is assumed that the surface electron scattering is diffuse. Interesting oscillatory structure appears in the absorptance for a thin film when the frequency is in the range $0.01\omega_p$–$0.1\omega_p$, where ω_p is the plasma frequency. The origin of this structure is discussed. An expression is derived for the absorptance of a thick sample in the infrared.

I. INTRODUCTION

Significant progress has been made of late in incorporating nonlocality into the theory of the optical properties of metals.[1–6] These studies, in which the electron scattering at the surface has either implicitly or explicitly been taken to be specular, have, in general, involved extensions of the pioneering work of Reuter and Sondheimer,[7] Dingle,[8] and Mattis and Dresselhaus[9] to include arbitrary incident angles[1,3,5] and/or finite thickness samples.[2–4,6]

There is now considerable evidence that a more generally valid description of the optical properties of metals is afforded by considering the surface electron scattering to be diffuse rather than specular. That is not to say that specular scattering does not occur. Indeed, for some materials, surfaces can be prepared in such a way that the desired degree of specular reflection can be ob-